Evolution and Control of Complex Curved Form in Simple Inorganic Precipitation Systems

ARTICLE *in* CRYSTAL GROWTH & DESIGN · JULY 2012

Impact Factor: 4.89 · DOI: 10.1021/cg3004646

6 AUTHORS, INCLUDING:

Matthias Kellermeier
BASF SE
56 PUBLICATIONS **569** CITATIONS
SEE PROFILE

Emilio Melero García
44 PUBLICATIONS **391** CITATIONS
SEE PROFILE

Melanie Pretzl
University of Bayreuth /Chemie Cluster Bayer…
11 PUBLICATIONS **116** CITATIONS
SEE PROFILE

Andreas Fery
Leibniz Institute of Polymer Research Dresden
251 PUBLICATIONS **4,850** CITATIONS
SEE PROFILE

CRYSTAL GROWTH & DESIGN

Article

pubs.acs.org/crystal

Evolution and Control of Complex Curved Form in Simple Inorganic Precipitation Systems

Matthias Kellermeier,[†,⊥] Josef Eiblmeier,[†] Emilio Melero-García,[‡] Melanie Pretzl,[§] Andreas Fery,[§] and Werner Kunz*[,†]

[†]Institute of Physical and Theoretical Chemistry, University of Regensburg, Universitätsstrasse 31, D-93040 Regensburg, Germany

[‡]Laboratorio de Estudios Crystalográficos, IACT (CSIC-UGR), Avda. del Conocimiento s/n, P.T. Ciencias de la Salud, E-18100 Armilla, Spain

[§]Physical Chemistry Department, University of Bayreuth, Universitätsstrasse 30, D-95445 Bayreuth, Germany

Supporting Information

ABSTRACT: Crystal architectures delimited by sinuous boundaries and exhibiting complex hierarchical structures are a common product of natural biomineralization. However, related forms can also be generated in purely inorganic environments, as exemplified by the existence of so-called "silica-carbonate biomorphs". These peculiar objects form upon coprecipitation of barium carbonate with silica and self-assemble into aggregates of highly oriented, uniform nanocrystals, displaying intricate noncrystallographic morphologies such as flat sheets and helicoidal filaments. While the driving force steering ordered mineralization on the nanoscale has recently been identified, the factors governing the development of curved forms on global scales are still inadequately understood. In the present work, we have investigated the circumstances that lead to the expression of smooth curvature in these systems and propose a scenario that may explain the observed morphologies. Detailed studies of the growth behavior show that morphogenesis takes crucial advantage of reduced nucleation barriers at both extrinsic and intrinsic surfaces. That is, sheets grow in a quasi-two-dimensional fashion because they spread across interfaces such as walls or the solution surface. In turn, twisted forms emerge when there is no foreign surface to grow on, such that the evolving aggregates curve back on themselves in order to use their own as a substrate. These hypotheses are corroborated by experiments with micropatterned surfaces, which show that the morphological selection intimately depends on the topology of the offered substrate. Finally, we demonstrate that, with the aid of suitable template patterns, it is possible to directly mold the shape (and size) of silica biomorphs and thus gain polycrystalline materials with predefined morphologies and complex structures.

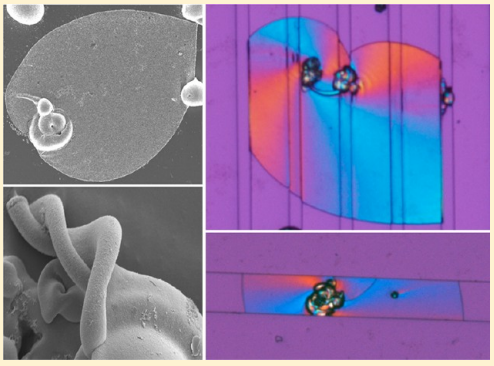

1. INTRODUCTION

In recent years, interest in polycrystalline aggregates comprising ordered arrays of miniaturized building blocks has been fuelled due to their relevance for diverse fields of research. Archetypes for these materials frequently occur in the course of biomineralization, where concerted assembly of small crystal components into higher-order architectures is a well-established strategy to produce inorganic matter with complex morphology, hierarchical structure, and superior properties.[1] This mode of construction is facilitated by the beneficial influence of an organic matrix on the crystallization process, which may control nucleation and growth of the crystallites, enable their stabilization, and direct oriented attachment of individuals.[2] Modern approaches of morphosynthesis are often meant to mimic the concepts observed in vivo, so as to design novel materials and at the same time shed light on the physicochemical principles underlying the biological process.[3] In particular, crystallization reactions involving a nonclassical pathway, along which crystal growth is driven by aggregation of nanoparticle units instead of ion-by-ion addition,[4] were found to be readily modified under certain conditions and thereby exploited to generate manifold superstructures.[5] For this purpose, organic additives are usually employed that are capable of interacting with the particles, stabilizing them at colloidal dimensions and thus preventing fusion to continuous single crystals. In this case, self-organization of the as-formed building blocks on the mesoscale, guided to a greater or lesser extent by the chemistry of the adsorbed additive, can yield in polycrystalline assemblies with delicate morphologies free of crystallographic symmetry,[6] especially when the primary units are featured by high shape anisotropy.[7] Such biomimetic modulations of classical crystallization scenarios were realized successfully, among many others, for calcium and barium carbonate with the aid of specialized block copolymers.[8]

Received: April 5, 2012
Revised: May 31, 2012
Published: June 6, 2012

   dx.doi.org/10.1021/cg3004646 | *Cryst. Growth Des.* 2012, 12, 3647−3655

The formation of crystal aggregates as those described above is however neither restricted to biological systems nor is it bound to the presence of organic substances, but can also be induced in purely inorganic environments. Indeed, simply by precipitating barium carbonate (witherite) in silica-rich media (either gel or solution) at elevated pH, a variety of complex crystal architectures are obtained which all delineate smoothly curved surfaces and hence, by intuition, yet misleadingly suggest biogenic origin.[9−12] These so-called silica−carbonate biomorphs spontaneously adopt intricate morphologies such as regular helicoids or sheets, which can grow to dimensions of several hundreds of micrometers. The internal structure of the precipitates is characterized by reams of uniform orthorhombic crystallites with a common elongated pseudohexagonal shape.[13−16] The orientation of these nanorods follows a distinct long-range order throughout the aggregate, with adjacent crystallites maintaining a slight misalignment and thus describing an orientational field with constantly varying vector.[13] In addition, individual rods as well as the whole assembly happen to be enveloped by skins of amorphous silica, rendering these materials dual composites with apparent intergrowth of species over multiple length scales.[17−20]

Though discovered already more than 30 years ago, central morphogenetic aspects of silica biomorphs have remained puzzling until recently. Work of García-Ruiz et al. revealed that the growth process divides into two fundamental stages, which are run through sequentially on the basis of temporally changing conditions.[21,22] First, a micrometer-sized crystal seed is formed, which becomes subject to self-similar branching due to crystal growth poisoning provoked by silica oligomers.[23] The result of this fractal route is a more or less closed spherulitic architecture, which can no longer grow as silica adsorption eventually locks up any active sites for further addition of carbonate units. Since the supersaturation is high at this time,[16] a multitude of new nuclei are generated all over the surface of the fractal aggregate. This causes fragmentation of the front and marks the beginning of the second stage of morphogenesis, which is characterized by polycrystalline growth. During this stage, evolving crystallites quickly become covered by silica, owing to local polymerization triggered by a decrease of pH in the vicinity of carbonate particles growing in alkaline media.[24] This prevents the crystallites from further growth and stabilizes them at nanoscale dimensions. However, as silica condensation proceeds, the pH becomes re-elevated nearby the front, such that the local carbonate supersaturation increases and novel events of nucleation occur. Overall, the pH-based coupling of the chemistry of carbonate and silicate initiates a loop process, during which components are alternately mineralized and a polycrystalline aggregate is formed.[21,25]

While this dynamic interplay steers growth on a microscopic level, still more delicate factors appear to govern the morphological evolution of the crystal aggregate toward sinuous shapes on a global scale. Previous studies have illustrated that self-assembly of the nanocrystals results at first in quasi-two-dimensional (2D) laminar forms with radial symmetry that sprout outward from their parent fractal spherulite.[11,21] The emergence of curvature and the concurrent formation of characteristic helicoidal or worm-like filaments were in turn ascribed to a singular curling at some point around the rim of the sheets and its subsequent propagation along their perimeter.

Although much has been learned in the past few years about the mechanisms underlying morphogenesis of silica biomorphs, there are still fascinating issues left to be explained.[26] For example, the reason why the polycrystalline assembly initially prefers to grow in the form of flat sheets, rather than in three dimensions, has so far not been clarified. Beyond that, little is known about the physical origin of smooth curvature in these plain inorganic systems — that is, the actual circumstances which provoke curling of the sheets. In the present work, we have sought answers to these questions by re-evaluating in detail the growth behavior of the aggregates and quantifying the yield of the different morphologies obtained from a typical experiment. Our results allow us to put forward a hypothesis that may rationalize the evolution of complex curved forms in these systems. Moreover, the proposed scenario would implicate a straightforward means to control the shape of the crystal aggregates, which is confirmed by experiments with micropatterned substrates as discussed in the second part of the paper.

2. EXPERIMENTAL SECTION

2.1. Synthesis and Characterization of Silica Biomorphs. In this work, silica biomorphs were grown exclusively from stagnant solutions, according to a protocol described previously.[15] Briefly, an adequate alkaline silica sol was prepared by diluting fresh commercial water glass stock (Sigma-Aldrich, reagent grade, containing 13.8 wt % Na and 12.5 wt % Si) 1:350 (v/v) with water. The equilibrated solution was subsequently mixed with 0.1 M NaOH (Merck, p.a.) in a ratio of 20:1 (v/v), such that a pH of about 11.3 was achieved. Crystallization was initiated by combining 5 mL of the sol rapidly with the same volume of a 0.01 M solution of barium chloride dihydrate (Sigma-Aldrich, ≥ 99.0%) in wells of a Nunc polystyrene multidish plate, having an area of 9.5 cm^2 and a depth of 1.7 cm. The final reaction mixtures thus had a starting pH of 11.1 ± 0.1 and species concentrations of 5 mM Ba^{2+}, 8.4 mM "SiO_2" and 8.9 mM Na^+. Manipulations and experiments were done at a constant temperature of 20 ± 1 °C. All solutions were prepared using water of Milli-Q quality and stored in tightly stoppered plastic bottles so as to avoid, at the high pH, undesired ingestion of both additional silica from glass walls and acidic carbon dioxide from the atmosphere prior to growth start.

Growth of mature silica biomorphs usually takes about 8−10 h at the given concentrations.[16] Aggregates are then seen to either float on the surface or adhere to the walls of the dishes. In this work, all experiments were aborted after a reaction time of 8 h by carefully removing the mother liquor. Because of the significant decrease of the bulk pH in the course of crystallization, amorphous silica also precipitated independently of the biomorphs and frequently buried the crystal aggregates on the bottom of the wells. Since all biomorphic structures were stuck tightly on the walls, they could easily be cleaned by repeatedly filling the wells with water, dispersing the silica floccules, and withdrawing them with a pipet. Eventually, the aggregates were washed several times with ethanol (Baker, p.a.) and left to dry in air. Formed precipitates were studied first by means of polarized light microscopy directly in the wells, using Nikon AZ100 and Eclipse E400 microscopes. Samples for scanning electron microscopy (SEM) were prepared readily by placing a small piece of conducting foil on the bottom of the well, rinsing the biomorphs grown on the substrate carefully, and mounting the dried foil directly on a SEM stub. After gold- or carbon-coating, specimens were inspected with a Jeol JSM 840 or a Zeiss LEO Gemini 1530 microscope. Suitable samples for atomic force microscopy (AFM) were obtained in a similar manner, but using glass coverslips instead of the conducting foil. Analyses were performed on a commercial AFM (NanoWizard, JPK Instruments, Germany), equipped with Si cantilevers having a force constant of 40 N/m (NSC 15, MicroMash, Estonia, resonant frequency: 325 kHz).

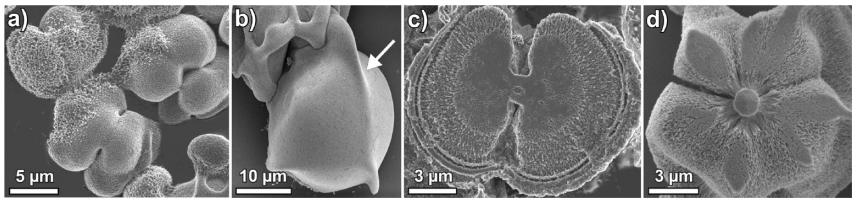

Figure 1. Fractal branching: during the first stage of the formation of silica biomorphs, a micrometer-sized elongated crystal becomes split at its ends under the poisoning influence of oligomeric silicate species. Continued branching at noncrystallographic angles ultimately results in globular structures (a, b), encompassing the original pseudohexagonal seed (c, d). The shown aggregates were isolated after 2 h of growth.

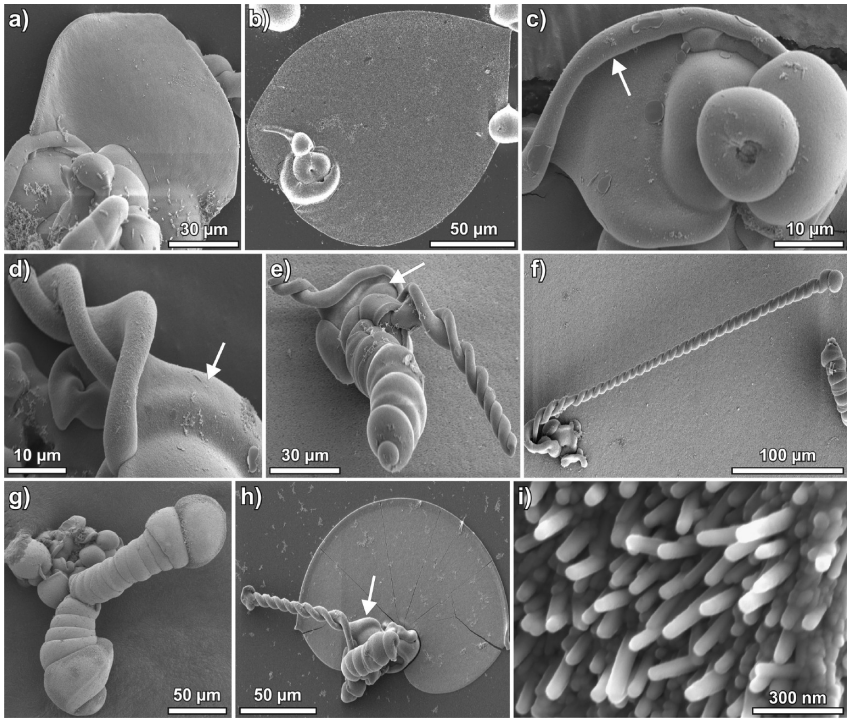

Figure 2. Polycrystalline growth: the second stage of morphogenesis is characterized by the development of various noncrystallographic morphologies, which fall into three major classes: extended flat sheets (a–c, h), helicoidal filaments (d–f, h), and worm-like braids (e, g, h). All of these forms emerge more or less directly from globular clusters and consist of uniform co-oriented nanorods, as evidenced by a zoom onto the surface of a sheet (i). Note that larger sheets always adhere tightly to the substrate surface over their entire area. Arrows in (d), (e), and (h) indicate small laminar sections which sprouted freely into the solution without contact to a surface, thus curled and gave rise to a helicoid soon.

Under the chosen conditions, the observed polycrystalline morphologies divide into three distinct types, namely, flat sheets, helicoidal filaments, and more tightly wound worm-like threads. Their relative occurrence was determined by counting aggregates of a given morphology on a predefined area in a series of independent experiments, as described in detail elsewhere.[25]

2.2. Fabrication of Micropatterned Substrates. Surfaces with defined periodic topology were obtained by manufacturing a polymeric replica of lithographically processed molds. For this purpose, silicon masters exhibiting different micrometer-scale structural motifs were purchased from GeSiM (Grosserkmannsdorf, Germany) and used to prepare stamps consisting of poly(dimethylsiloxane) (PDMS) following a procedure reported in the literature.[27] First, masters were hydrophobized by treatment with (heptadecafluoro-1,1,2,2-tetrahydrodecyl)-dimethylchlorosilane (ABCR Specialty Chemicals) to ensure removability of the PDMS stamp after completed preparation. Then, polymer precursor solution made by mixing Sylgard 184 (prepolymer received from Dow Corning) and a curing agent in a mass ratio of 10:1 was cast onto the masters. After degassing in a vacuum, samples were cured for 12 h at 60 °C. Eventually, the templated polymeric matrix was detached from the mold and hydrophilized in oxygen plasma for 45 s at 0.2 mbar and an intensity of 80 W, using a Flecto10 instrument from Plasma Technology.

Growth of silica biomorphs on as-prepared micropatterned surfaces was realized by placing the PDMS stamps into wells, filling with reaction mixture, and withdrawing the substrate from the solution after a growth period of 8 h with a pair of tweezers. Formed aggregates could readily be cleaned by careful rinsing with water and ethanol, and were studied by optical microscopy and SEM while still attached to the substrate.

3. RESULTS AND DISCUSSION

3.1. Morphogenesis of Silica Biomorphs in Solutions. When allowing the alkaline mixtures to equilibrate under quiescent conditions in contact with the atmosphere, continuous diffusion of carbon dioxide into the system and its conversion to carbonate species gradually lower the pH, from initially about 11.1 to 10.2 after 8 h. In parallel, the supersaturation of barium carbonate increases and crystallization sets in usually within less than 2 h. Crystal aggregates isolated at the end of the experiments were widely identical in terms of morphology, size, and structure to those described in previous studies dealing with solutions at similar concentrations

dx.doi.org/10.1021/cg3004646 | Cryst. Growth Des. 2012, 12, 3647–3655

and pH.[11−14,16,21,23,25] SEM images of characteristic forms are shown in Figures 1 and 2.

Particles retrieved from their mother liquor already after a few hours of growth display primarily deformed globular or partially open spherulitic shapes (Figure 1a,b), and frequently agglomerate to larger clusters. The core of these globules consists of an elongated pseudohexagonal crystal, typically around 1−2 μm wide (Figure 1c,d), which nucleated heterogeneously at either the solution surface or the walls of the used vessel (as is evident from the flatness of the areas imaged in Figure 1c,d). Because of noncrystallographic branching at both of its ends,[21] this crystal first transforms into dumbbell-shaped structures, which then become closed to more or less spherical architectures by continued splitting (cf. Figure 1b).

At this point, the system passes into the stage where growth is based on the assembly of nanoscale units, presumably driven by the meanwhile elevated supersaturation of the solutions.[16] Thereby, crystallites initially happen to be attached only along a quite thin path over the surface of the globules (indicated by the arrow in Figure 1b). In the following, flat sheets with thicknesses in the range of 1−3 μm are extracted from the fractal precursors and grow radially in a quasi-2D fashion to adopt various rounded shapes (Figure 2a−c, h). After some time, these sheets develop scrolled margins (arrow in Figure 2c) and exhibit one or more cusps around their rim (cf. Figure 2b), owing to curling and the consequential competition between radial and tangential growth.[11,21] Helicoidal structures emerge when two such curls of equal handedness collide and intertwine, inducing a twist which is subsequently perpetuated by continued mutual winding (Figure 2d−f, h). Worm-like morphologies (Figure 2g) are in turn generated when a sheet curls and keeps on coiling on itself.[21] High-magnification SEM images (Figure 2i) confirm that all sheets, helicoids, and worms are indeed crystal aggregates consisting of oriented rod-like units about 200−300 nm long and 40−60 nm across, which is in fair agreement with values reported in the literature.[12,13,16,28]

Indeed, a morphogenetic scenario comprising the formation of extended sheets, which subsequently curl and twist to produce helicoidal filaments, depicts well the growth behavior of silica biomorphs typically observed in gels.[14,21,22] However, there is some deviance realized in the solution experiments of the present work that has not been mentioned to date and thus deserves attention. First, we note that virtually all flat sheets grew over their entire area in direct contact with either the surface of the wells or the solution−air interface (cf. Figure 2b,h). In fact, sheets formed on the walls adhered so firmly that they could hardly be loosened without breaking them. By contrast, helicoids and worms did not stick to surfaces, but protruded at arbitrary angles into the solution (Figure 2e−h). These considerations are supported by syntheses of silica biomorphs in stirred solutions, as described in a recent study.[25] Corresponding experiments showed that sheets could grow even at high stirring frequencies, whereas the formation of twisted morphologies was largely impeded. This finding was ascribed to the presence of quasi-stagnant boundary layers at interfaces, throughout which sheets could evolve along the surface without any noticeable perturbation. Worms and helicoids, in turn, grew protruding into the liquid and hence experienced significantly stronger fluid motion, which interfered with the coupled precipitation mechanism and thus prevented their formation.

Second, throughout the numerous experiments we have performed, there was not a single case in which a twisted filament sprouted from a sheet larger than a few micrometers. Rather, the sheets that give rise to helical forms were those which grew independently of a surface and hence curled soon after emerging from the globular clusters (arrows in Figure 2d,e,h mark corresponding sheet-like segments). Very often, the transformation of the initial leaf to a helicoid occurred almost immediately after polycrystalline growth had commenced, such that a distinct flat domain cannot be distinguished and the helicoid appears to emerge directly from its parent fractal aggregate (cf. Figure 2e,f). This holds true also for any worm-like morphology sighted in our studies. Here, winding always proceeded right from the beginning, leaving no space for an even section in-between (see Figure 2e,g).

Third, it is worth noting that by far not all fractal spherulites develop a sheet, a worm, or a helicoid. Instead, growth ends in many cases once self-similar branching is terminated. Figure 3 illustrates the relative occurrence of the different morphologies found in a typical experiment. The term "globules" thereby refers to any fractal aggregate which has not produced characteristic biomorphic forms. Evidently, this applies to almost 50% of the counted precipitates. Among the polycrystalline architectures, worms are clearly most frequent, while the fractions of sheets and helicoids amount to less than 10%.

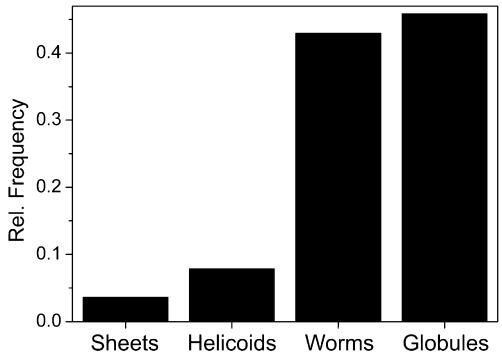

Figure 3. Statistical distribution of morphologies displayed by silica biomorphs grown in a typical solution experiment. Values were obtained by counting particles on a default area of the crystallization wells in a considerable number of independent experiments. Note that only those sheets were counted which did not give rise to a helical filament.

The observed morphological distribution can be rationalized when assuming that any sheet-like aggregate about to emerge from a fractal spherulite is prone to instant curling if it grows at a noticeable distance from a surface. Reasonably, the probability for the initial outgrowth of a nanocrystalline assembly from a given globule should be equal all over its surface. However, if this transition can only yield in extended sheets when taking place nearby the wall of the vessel (and, thus, at the bottom of the globule), the relatively rare occurrence of this kind of morphology can readily be understood. By nature, this is different in gels, since the silica matrix universally provides a surface to grow on throughout the sample in this case (assuming the gel to be a two-phase system with pores of liquid being surrounded by heavily condensed networks of silica). On the basis of the above hypothesis, these circumstances may well be responsible for the consistent formation of large and often slightly sinuous sheets in gels, whereas their

dx.doi.org/10.1021/cg3004646 | Cryst. Growth Des. 2012, 12, 3647−3655

solution counterparts are generally flat, much less abundant, and adhere to interfaces. Similar arguments can be put forward to explain the low number of helicoids discerned in the present experiments, as compared to worm-like structures. Worms are sheets which bend immediately after their initiation and wind around themselves in the following. The formation of helicoids, in turn, necessitates at least a short laminar domain which can curl and twist. However, as growth of even sheets seems to be generally unfavorable far off a surface, and since a sheet cannot curl downward when growing flat in contact with an interface, the preconditions required for the generation of a helical filament are rather seldom fulfilled. Therefore, worms are the most frequent polycrystalline morphology in a solution experiment. As opposed to that, practically all gel-grown aggregates have developed extended sheets before curling, such that the formation of helicoids becomes strongly favored and worms are hardly ever observed.[14,22]

In light of these findings, we propose that the morphogenesis of silica biomorphs is intimately related to the presence of both extrinsic and intrinsic surfaces. As long as growth of the polycrystalline assembly proceeds close to a foreign surface, like well walls in a solution experiment or the silica matrix in a gel setup, it will adopt the topology of the substrate by covering its surface with a thin layer of crystallites. The reason for this surface affinity and the concurrent quasi-2D growth behavior most likely relies on reduced nucleation barriers prevailing at interfaces (i.e., heterogeneous nucleation). In the absence of such a substrate, the only surface available for the aggregates to grow on is their own. In fact, biomorphs do even appear to have some sort of affinity for their own surface as a growth substrate, as becomes manifest in the finding that new aggregates often form in close contact on top of already existing ones (see Figure S1 in the Supporting Information (SI)). Thus, when a sheet is about to evolve freely in a solution (or once it encounters any discontinuity in the silica matrix during formation in gels), it will prefer curved growth and curl in order to fold back on itself and facilitate further nucleation. Depending on the actual conditions, the induced curling can affect either an emerging sheet as a whole, thus resulting in worm-like braids, or trigger ongrowth of a wave-like lip along the sheet perimeter leading to helicoidal filaments. In this sense, the initial two-dimensionality as well as the origin of curvature and twisted structures in these systems could derive to a greater or lesser extent from the beneficial impact of surfaces on nucleation scenarios.

3.2. Shaping Silica Biomorphs. Such a morphogenetic scenario inevitably implies that silica biomorphs should be sensitive to the properties and condition of the surface they grow on. To verify this hypothesis, we performed experiments with substrates having a defined and noneven topology. For this purpose, surfaces exhibiting a line-pattern microstructure of periodically arranged, rectangular division bars were employed. While the height of these bars was kept constant at 5 μm, their width (w) and mutual distance (d) were varied. Detailed studies of the samples showed that the latter two parameters, and in particular the dimensions of the indents between the bars, essentially affect the morphological evolution of the aggregates, as described in the following.

When both w and d were set to 5 μm (Figure 4), nucleation of crystal seeds was found to occur almost exclusively on top of the bars, presumably due to the limited space in the gaps and the poor accessibility of the enclosed volume. Fractal branching then produced variously shaped and intergrown globular

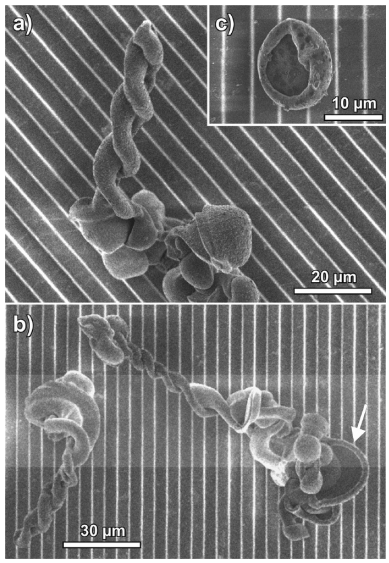

Figure 4. SEM images of biomorphs grown on a polymeric substrate exhibiting a regular line-pattern topology with $w = d = 5$ μm. The uneven relief of the surface on the micrometer-scale impedes the formation of extended flat sheets and causes emerging laminar segments to curl soon. Consequently, helicoids and worms protruding from the surface represent the major fraction of aggregates observed in the experiments.

clusters, which often extended over several bars bridging the indents (cf. Figure 4a,b). Notably, the distribution of polycrystalline morphologies formed on the patterned substrate differed drastically from what is usually observed on even surfaces. In fact, we could not discern any regular sheet that grew flat over distances larger than 10 μm. Instead, the vast majority of aggregates obtained under these conditions were worms and helicoids protruding steeply from the surface (Figure 4a,b). The few laminar segments sighted were in turn heavily scrolled around their rim (see arrow in Figure 4b).

It is worth emphasizing that these differences in the growth behavior are not related to the chemical nature of the surface. Indeed, we found spacious sheets in unstructured parts of the polymeric base, occasionally right next to patterned regions (see Figure S2 in the SI). Additional experiments with other materials as substrates (distinct polymers, glasses, and metals) further proved that the surface composition has no noticeable effect on morphogenesis. This confirms that the given topologies alone provoked the observed changes (and that there is no significant influence of the particular water structure nearby interfaces, either). Comparable results were moreover achieved when a pattern with distinct geometry, but similar structural dimensions was used (see Figure S2 in the SI).

The above findings are perfectly in line with the proposed model of surface-assisted mineralization. A sheet which emerges from its fractal precursor may grow on the top face of the bar but, when arriving at the gap, starts to curl (Figure 4c). The abrupt vertical change of the topology at this point can obviously not be followed by the crystal assembly, such that curved growth back toward the own surface is preferred. Likewise, the distance between the bars is apparently too large to be covered by the sheet without an underlying substrate, although this seems to be sporadically possible (Figure 4b). As a consequence, twisted morphologies and worm-like braids become strongly favored over extended flat sheets on the micropatterned surface. In this regard, modifying the structural

dx.doi.org/10.1021/cg3004646 | Cryst. Growth Des. 2012, 12, 3647−3655

constitution of the growth substrate represents a straightforward means to influence the formation of silica biomorphs and, in particular, the yield of specific morphologies.

However, we also observed exceptions to this typical mode of growth on line patterns with d = 5 μm (Figure 5). For instance,

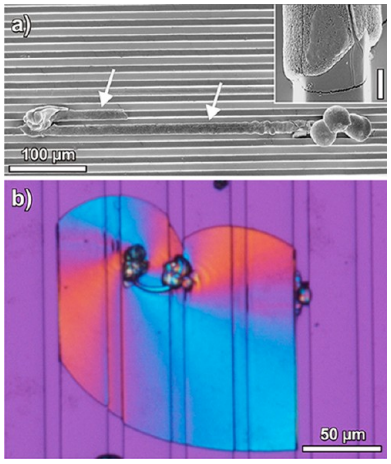

Figure 5. Novel forms of silica biomorphs obtained upon growth on micropatterned substrates. (a) SEM image showing crystal aggregates which spread across the top face of a division bar over fairly large distances (w = d = 5 μm). Inset: close-up view of the edge of such an aggregate, demonstrating that it grew around the corner of the bar and covered also its side faces (scale bar: 2 μm). (b) Polarized optical micrograph of a sheet that extends over several elevations and gaps while maintaining close contact to the underlying surface and hence replicating the topology of the substrate (w = 30 μm, d = 10 μm).

sheets were sometimes seen to become extruded from globular clusters on top of a bar and subsequently cover its surface over distances of up to several hundreds of micrometers, thus adopting intricate rectangular shapes (Figure 5a). A closer look at one such aggregate reveals that also the side faces of the bar were coated by the crystal assembly in this case (inset in Figure 5a). This implies that, although common, curling does not necessarily have to occur at the edge of a bar and sheets are indeed capable of bending around sharp corners occasionally. An even more intriguing example supporting this notion is depicted in Figure 5b. Here, a sheet has grown over a couple of bars and indents — always in direct contact with the substrate surface — until its formation was terminated at an edge on both sides, giving a patterned crystal aggregate delimited by straight boundaries (instead of the curved perimeters usually displayed by silica biomorphs). Moreover, the observed color interference patterns resemble those of biomorph sheets formed on even surfaces,[13] indicating that the edged profile of the substrate did not affect the microstructure of the aggregate. Although we cannot certainly identify the factors that decide whether a sheet curls at an edge or is able to follow the topology of the substrate, we suspect that a key parameter in this context is the actual growth rate of the aggregate, which has been reported to vary from aggregate to aggregate in a given batch.[16] Possibly, sheets that evolve rather slowly manage to change their growth direction in an orthogonal fashion at the rim of a bar, whereas those which grow faster prefer folding back on their own surface.

In any case, these observations suggest that both the shape and topology of silica biomorphs can be tuned by using suitable micropatterned growth substrates. Indeed, still more sophisticated control over morphology can be achieved when the distance between the division bars is increased. For d-values equal to or larger than 10 μm, nucleation of crystal seeds is no longer prevented in the gaps between the bars. Furthermore, there is apparently enough space in the indents allowing for an unimpeded development of fractal globules, which subsequently give rise to polycrystalline structures. The evolution of the emerging aggregates is now drastically affected by the substrate (Figure 6).

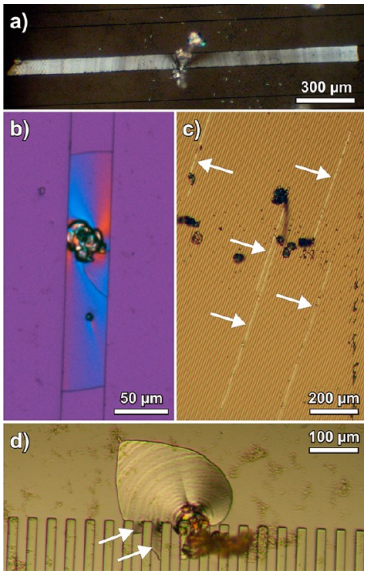

Figure 6. Templating silica biomorphs. (a–c) Growth on line patterns with bar distances ≥ 10 μm results in quasi-rectangular stripe-like morphologies, as emerging laminar aggregates become molded into the indents between the bars. (d) Optical micrograph of a sheet formed right at the border of the patterned area. It is evident that the crystal assembly tends to dodge obstacles and continues growing only along flat pathways, such that it penetrates the channels from the outside (arrows) and encloses the bar ends. Substrate dimensions: (a) w = 160 μm, d = 80 μm, (b) w = 100 μm, d = 40 μm, (c) w = 10 μm, d = 10 μm, (d) w = 20 μm, d = 20 μm.

We find that sheets grow on the bottom of the indents and follow the direction of the channels across the surface, whereas their lateral expansion is confined by the walls of the bars on both sides. In this manner, peculiar elongated, stripe-like morphologies are formed in a direct molding process, partially reaching lengths in the millimeter range (see Figure 6a–c and Figure S3 in the SI for more images). The fact that sheets commonly cease to grow when arriving at the bar walls becomes comprehensible when considering their typical height: AFM analyses of a representative aggregate gave an approximate mean thickness of around 0.65 μm (see Figure S4 in the SI), which is small as compared to the height of the bars (5 μm). Therefore, the bars pose a serious obstacle for evolving sheets, and termination of growth at their walls is obviously favored over an abrupt change of the direction in the majority of cases.

Extinction patterns observed when viewing these quasi-rectangular aggregates between crossed polarizers suggest radial orientation of the constituting crystallites from the central globular particle outward (Figure 6b), in line with what has been reported for growth in the absence of a patterned surface.[13] This shows that the molded sheets may exhibit an

dx.doi.org/10.1021/cg3004646 | Cryst. Growth Des. 2012, 12, 3647–3655

orientational ordering of building units on the mesoscale that is comparable to the structure of nontemplated counterparts and has thus not suffered from the spatial constraints imposed during morphogenesis (although this does not apply to all investigated specimens, cf. Figure S3 in the SI). Further, it is worth noting that imprinting of a stripe-like shape on the growing biomorphs was not a rare event under these conditions, in contrast to the forms displayed in Figure 5. Among the fraction of aggregates that grew in the gaps between bars, morphologies like those depicted in Figure 6a,b were indeed the rule rather than exceptions for substrates with $d \geq 10$ μm, as illustrated by Figure 6c. This is clearly beneficial when it comes to the concerted synthesis of ordered crystal assemblies with controlled shape and size. Finally, it shall be mentioned that molding of sheets can also occur when morphogenesis is initiated in unstructured regions of the polymeric base, but still close to the periodic pattern. In such a case (Figure 6d), the aggregate evolves ordinarily until it encounters the ends of the bars. At this point, uniform radial advancement is disrupted by the substrate topology and the front splits in order to shun elevated parts of the surface. Growth then proceeds selectively along directions where the substrate remains flat. That is, the sheet infiltrates the channels of the pattern, thus encasing multiple bars in its overall structure. Occasionally, we also found an inverse scenario where a sheet became extruded from a fractal globule within one of the channels and, upon growth, reached the borderline of the patterned area (see Figure S5 in the SI). Interestingly, the laminar aggregate abandoned its rectangular morphology and began to spread equally in all directions once it had left the channel, eventually adopting a characteristic leaf-like shape, which is the typical product of sheet growth on even surfaces.[21] In addition, this particular sheet formed on top of a larger one, which had grown right at the rim of the patterned area and intruded into the neighboring channel, yielding a stripe-like architecture several hundreds of micrometers in length (cf. Figure S5 in the SI). These curious observations highlight the flexibility of the mechanism driving the formation of silica biomorphs on the one hand, while, on the other, they underline the pivotal role of (extrinsic) surfaces in the progress of morphogenesis. Taken together, the experiments described above provide clear evidence that the shape of silica biomorphs can be directly molded by applying micropatterned substrates as templates.

We note that the morphologies shown in Figure 6 resemble to some degree calcium carbonate structures prepared by Kim et al., who used a polymer-induced liquid precursor (PILP) phase to mineralize a square array of cross-linked channels, the surface of which was functionalized with self-assembled monolayers (SAMs).[29] Preferential deposition of PILP droplets on the monolayers led to the formation of a continuous liquid-like mineral film which, upon solidification and crystallization, transformed into patterned 2D calcite crystals comprising extended single-crystalline domains (50−100 μm). In a previous study, Aizenberg et al. demonstrated that by filling the interstices of a micropatterned framework with metastable amorphous calcium carbonate (ACC), millimeter-sized single crystals of calcite with defined orientation and periodic holes can be obtained if nucleation is initiated and controlled by a SAM-decorated nanoregion.[30] Beyond that, also three-dimensional single-crystalline architectures exhibiting complex non-crystallographic shapes and distinct microstructural features could be realized via such templating approaches, for instance, with the aid of polymeric sea urchin plate replicas[31] or by infiltrating ACC dispersions into colloidal−crystal assemblies.[32] The structures obtained in the present work obviously differ from those mentioned above by the fact that they are polycrystalline. However, unlike typical polycrystalline films, our molded sheets consist of uniform nanosized building units that follow a specific long-range order on the mesoscale — as a consequence of the growth mechanism innate to silica biomorphs. In this regard, we have successfully combined top-down templating of shape by means of a confined reaction space with bottom-up self-assembly of elaborate textures through a dynamic interplay of simple components. Such a scenario may well mirror the strategies applied by biomineralization to create materials of outstanding complexity.

4. SUMMARY AND CONCLUSIONS

Silica biomorphs resemble polycrystalline biominerals in terms of structural hierarchy, oriented texture, and smoothly curved morphologies without being biomimetic in the true sense, as their formation does not require organic matrices or polymeric additive molecules. Given the ease of preparation, these materials yet serve as model systems for studying the directed self-organization of nanoscale building units in general. Understanding the mechanisms that trigger structure evolution in this case could help to gain deeper insight to the concepts at work during biomineralization and may devise new approaches for laboratory morphosynthesis.

The results of the present work have shed novel light on the development of the crystal aggregates on global scales and led to a feasible explanation for the characteristic quasi-two-dimensionality of sheets and the actual origin of curvature. The collected data suggest that growth of silica biomorphs is closely linked to the presence of surfaces which facilitate nucleation. In solutions, aggregates form exclusively via heterogeneous nucleation at interfaces, and sheets expand to larger dimensions only when growing flat in contact with for instance a wall. Curved and twisted structures such as helicoids or worms emerge by contrast when polycrystalline growth is initiated far from an interface, such that the assembly needs to turn back in order to use, for lack of an extrinsic surface, its own as substrate.

A direct implication of these hypotheses is that it should be possible to influence morphogenesis of silica biomorphs by varying the topology of the surface they grow on. Experiments with microstructured substrates exhibiting line-pattern profiles of periodically changing height confirmed this notion and proved that the physical dimensions of the imposed pattern essentially determine the effect on the growth process. When the distance between the division bars on the surface is too small to allow for nucleation in the indents, growth occurs only on top of the bars, and emerging laminar aggregates usually curl once they arrive at the edge, thus rendering the formation of extended sheets largely impeded. In parallel, the amount of helicoids and worms — which arise as a result of sheet curling and grow protruding into the solution — is dramatically increased relative to reference samples. This validates the crucial role of extrinsic surfaces during morphogenesis and shows that the fractions of distinct morphologies in a given batch can be tuned concertedly. On the other hand, substrates with larger dimensions (i.e., greater distances in-between bars) enable nucleation and growth also in the indents, such that flat sheets begin to spread over the bottom of the gaps in the pattern. However, since lateral expansion of the sheets is confined by the width of the indents while growth along the

channels remains unhindered, quasi-rectangular stripes are generated as the geometry of the substrate is imprinted on the developing crystal aggregate. These findings, along with other observations, demonstrate that the shape, size, and likely also curvature of silica biomorphs can be forthright molded, as a direct consequence of their "surface affinity". We envisage that by means of different substrates — for example surfaces with smooth, wavy profiles or patterns with indents of distinct geometry — further intriguing morphologies will be accessible.

■ ASSOCIATED CONTENT

Supporting Information

Additional SEM and optical micrographs of silica biomorphs formed on even as well as micropatterned surfaces (Figures S1−S5). This material is available free of charge via the Internet at http://pubs.acs.org.

■ AUTHOR INFORMATION

Corresponding Author

*E-mail: werner.kunz@chemie.uni-regensburg.de. Phone: (+49) 941 943 4044. Fax: (+49) 941 943 4532. Web: www-kunz.chemie.uniregensburg.de.

Present Address

[⊥]Physical Chemistry, University of Konstanz, Universitätsstrasse 10, D-78457 Konstanz, Germany.

Notes

The authors declare no competing financial interest.

■ ACKNOWLEDGMENTS

The authors thank Prof. Dr. Juan Manuel García-Ruiz (Laboratorio de Estudios Crystalográficos, CSIC-UGR) for valuable discussions. We are further grateful to Benjamin Gossler, Martina Heider and Werner Reichstein (University of Bayreuth) for access to their field-emission scanning electron microscope and help with the analyses. M.K. appreciates the granting of a scholarship by the Fonds der Chemischen Industrie. E.M.G. acknowledges financial support by the program Juan de la Cierva of the Spanish Science Ministry (MICINN).

■ REFERENCES

(1) (a) Lowenstam, H. A.; Weiner, S. *On Biomineralization*; Oxford University Press: New York, 1989. (b) Weiner, S.; Addadi, L. *J. Mater. Chem.* **1997**, *7*, 689. (c) Jodaikin, A.; Weiner, S.; Traub, W. *J. Ultrastruct. Res.* **1984**, *89*, 324. (d) Young, J. R.; Davis, S. A.; Bown, P. R.; Mann, S. *J. Struct. Biol.* **1999**, *126*, 195. (e) Rodriguez-Navarro, A. B.; Yebra, A.; Nys, Y.; Jimenez-Lopez, C.; Garcia-Ruiz, J. M. *Eur. J. Mineral.* **2007**, *19*, 391. (f) Gilbert, P. U. P. A.; Metzler, R. A.; Zhou, D.; Scholl, A.; Doran, A.; Young, A.; Kunz, M.; Tamura, N.; Coppersmith, S. N. *J. Am. Chem. Soc.* **2008**, *130*, 17519. (g) Robinson, C. *J. Dent. Res.* **2007**, *86*, 677.

(2) (a) Mann, S.; Archibald, D. D.; Didymus, J. M.; Douglas, T.; Heywood, B. R.; Meldrum, F. C.; Reeves, N. J. *Science* **1993**, *261*, 1286. (b) Falini, G.; Albeck, S.; Weiner, S.; Addadi, L. *Science* **1996**, *271*, 67. (c) Belcher, A. M.; Wu, X. H.; Christensen, R. J.; Hansma, P. K.; Stucky, G. D.; Morse, D. E. *Nature* **1996**, *381*, 56. (d) Albeck, S.; Weiner, S.; Addadi, L. *Chem.—Eur. J.* **1996**, *2*, 278. (e) Levi-Kalisman, Y.; Falini, G.; Weiner, S.; Addadi, L. *J. Struct. Biol.* **2001**, *135*, 8. (f) Veis, A. *Rev. Mineral. Geochem.* **2003**, *54*, 249. (g) Nudelman, F.; Gotliv, B. A.; Addadi, L.; Weiner, S. *J. Struct. Biol.* **2006**, *153*, 176.

(3) (a) Mann, S. *Biomineralization: Principles and Concepts in Bioinorganic Materials Chemistry*; Oxford University Press: New York, 2001. (b) Arias, J. L.; Fernández, M. S. *Mater. Charact.* **2003**, *50*, 189. (c) Oaki, Y.; Kotachi, A.; Miura, T.; Imai, H. *Adv. Funct. Mater.* **2006**, *16*, 1633. (d) Meldrum, F. C.; Cölfen, H. *Chem. Rev.* **2008**, *108*, 4332.

(4) (a) Banfield, J. F.; Welch, S. A.; Zhang, H.; Ebert, T. T.; Penn, R. L. *Science* **2000**, *289*, 751. (b) Polleux, J.; Pinna, N.; Antonietti, M.; Niederberger, M. *Adv. Mater.* **2004**, *16*, 436.

(5) (a) Cölfen, H.; Antonietti, M. *Angew. Chem., Int. Ed.* **2005**, *44*, 5576. (b) Mann, S. *Nat. Mater.* **2009**, *8*, 781. (c) Niederberger, M.; Cölfen, H. *Phys. Chem. Chem. Phys.* **2006**, *8*, 3271.

(6) (a) Li, M.; Schnablegger, H.; Mann, S. *Nature* **1999**, *402*, 393. (b) Bigi, A.; Boanini, E.; Walsh, D.; Mann, S. *Angew. Chem., Int. Ed.* **2002**, *41*, 2163. (c) Cölfen, H.; Qi, L.; Mastai, Y.; Börger, L. *Cryst. Growth Des.* **2002**, *2*, 191. (d) Shi, H. T.; Qi, L. M.; Ma, J. M.; Cheng, H. *J. Am. Chem. Soc.* **2003**, *125*, 3450. (e) Mukkamala, S. B.; Powell, A. K. *Chem. Commun.* **2004**, 918. (f) Gehrke, N.; Cölfen, H.; Pinna, N.; Antonietti, M.; Nassif, N. *Cryst. Growth Des.* **2005**, *5*, 1317. (g) Volkmer, D.; Harms, M.; Gower, L. B.; Ziegler, A. *Angew. Chem., Int. Ed.* **2005**, *44*, 639.

(7) Cölfen, H.; Mann, S. *Angew. Chem., Int. Ed.* **2003**, *42*, 2350.

(8) (a) Yu, S. H.; Cölfen, H.; Antonietti, M. *J. Phys. Chem. B* **2003**, *107*, 7396. (b) Wang, T.; Cölfen, H.; Antonietti, M. *J. Am. Chem. Soc.* **2005**, *127*, 3246. (c) Yu, S. H.; Cölfen, H.; Tauer, K.; Antonietti, M. *Nat. Mater.* **2005**, *4*, 51. (d) Wang, T.; Xu, A. W.; Cölfen, H. *Angew. Chem., Int. Ed.* **2006**, *45*, 4451. (e) Cölfen, H. *Top. Curr. Chem.* **2007**, *271*, 1.

(9) (a) Garcia-Ruiz, J. M.; Amoros, J. L. *J. Cryst. Growth* **1981**, *55*, 379. (b) Garcia-Ruiz, J. M. *J. Cryst. Growth* **1985**, *73*, 251.

(10) Garcia-Ruiz, J. M. *Origins Life Evol. Biosphere* **1993**, *24*, 451.

(11) Garcia-Ruiz, J. M.; Carnerup, A. M.; Christy, A. G.; Welham, N. J.; Hyde, S. T. *Astrobiology* **2002**, *2*, 353.

(12) Garcia-Ruiz, J. M.; Hyde, S. T.; Carnerup, A. M.; Christy, A. G.; Van Kranendonk, M. J.; Welham, N. J. *Science* **2003**, *302*, 1194.

(13) Hyde, S. T.; Carnerup, A. M.; Larsson, A. K.; Christy, A. G.; Garcia-Ruiz, J. M. *Physica A* **2004**, *339*, 24.

(14) Bittarello, E.; Aquilano, D. *Eur. J. Mineral.* **2007**, *19*, 345.

(15) Kellermeier, M.; Glaab, F.; Carnerup, A. M.; Drechsler, M.; Gossler, B.; Hyde, S. T.; Kunz, W. *J. Cryst. Growth* **2009**, *311*, 2530.

(16) Kellermeier, M.; Melero-Garcia, E.; Glaab, F.; Eiblmeier, J.; Kienle, L.; Rachel, R.; Kunz, W.; Garcia-Ruiz, J. M. *Chem.—Eur. J.* **2012**, *18*, 2272.

(17) Terada, T.; Yamabi, S.; Imai, H. *J. Cryst. Growth* **2003**, *253*, 435.

(18) (a) Imai, H.; Terada, T.; Miura, T.; Yamabi, S. *J. Cryst. Growth* **2002**, *244*, 200. (b) Voinescu, A. E.; Kellermeier, M.; Bartel, B.; Carnerup, A. M.; Larsson, A. K.; Touraud, D.; Kunz, W.; Kienle, L.; Pfitzner, A.; Hyde, S. T. *Cryst. Growth Des.* **2008**, *8*, 1515.

(19) Voinescu, A. E.; Kellermeier, M.; Carnerup, A. M.; Larsson, A. K.; Touraud, D.; Hyde, S. T.; Kunz, W. *J. Cryst. Growth* **2007**, *306*, 152.

(20) Bittarello, E.; Massaro, F. R.; Aquilano, D. *J. Cryst. Growth* **2010**, *312*, 402.

(21) Garcia-Ruiz, J. M.; Melero-Garcia, E.; Hyde, S. T. *Science* **2009**, *323*, 362.

(22) Melero-Garcia, E.; Santisteban-Bailon, R.; Garcia-Ruiz, J. M. *Cryst. Growth Des.* **2009**, *9*, 4730.

(23) Garcia-Ruiz, J. M. *Geology* **1996**, *26*, 843.

(24) Kellermeier, M.; Melero-Garcia, E.; Glaab, F.; Klein, R.; Drechsler, M.; Rachel, R.; Garcia-Ruiz, J. M.; Kunz, W. *J. Am. Chem. Soc.* **2010**, *132*, 17859.

(25) Kellermeier, M.; Melero-Garcia, E.; Kunz, W.; Garcia-Ruiz, J. M. *J. Colloid Interface Sci.* **2012**, DOI: 10.1016/j.jcis.2012.05.009.

(26) Kunz, W.; Kellermeier, M. *Science* **2009**, *323*, 344.

(27) Pretzl, M.; Schweikart, A.; Hanske, C.; Chiche, A.; Zettl, U.; Horn, A.; Böker, A.; Fery, A. *Langmuir* **2008**, *24*, 12748.

(28) Hyde, S. T.; Garcia-Ruiz, J. M. *Actual. Chim.* **2004**, *275*, 4.

(29) Kim, Y.-Y.; Douglas, E. P.; Gower, L. B. *Langmuir* **2007**, *23*, 4862.

(30) (a) Aizenberg, J.; Muller, D. A.; Grazul, J. L.; Hamann, D. R. *Science* **2003**, *299*, 1205. (b) Aizenberg, J. *Adv. Mater.* **2004**, *16*, 1295.

(31) (a) Park, R. J.; Meldrum, F. C. *Adv. Mater.* **2002**, *14*, 1167. (b) Park, R. J.; Meldrum, F. C. *J. Mater. Chem.* **2004**, *14*, 2291.

(c) Wucher, B.; Yue, W.; Kulak, A. N.; Meldrum, F. C. *Chem. Mater.* **2007**, *19*, 1111.
(32) Li, C.; Qi, L. *Angew. Chem., Int. Ed.* **2008**, *47*, 2388.